

Optimizing traffic flow using quantum annealing and classical machine learning

Florian Neukart^{*1}, Gabriele Compostella², Christian Seidel², David Von Dollen¹,
Sheir Yarkoni³, and Bob Parney³

¹Volkswagen Group of America

²Volkswagen Data:Lab

³D-Wave Systems, Inc.

Abstract

Quantum annealing algorithms belong to the class of meta-heuristic tools, applicable for solving binary optimization problems. Hardware implementations of quantum annealing, such as the quantum processing units (QPUs) produced by D-Wave Systems [1], have been subject to multiple analyses in research, with the aim of characterizing the technology's usefulness for optimization and sampling tasks [2–15]. In this paper, we present a real-world application that uses quantum technologies. Specifically, we show how to map certain parts of the real-world traffic flow optimization problem to be suitable for quantum annealing. We show that time-critical optimization tasks, such as continuous redistribution of position data for cars in dense road networks, are suitable candidates for quantum applications. Due to the limited size and connectivity of current-generation D-Wave QPUs, we use a hybrid quantum and classical approach to solve the traffic flow problem.

^{*}Corresponding author: florian.neukart@vw.com

1 Introduction

Quantum annealing technologies such as the quantum processing units (QPUs) made by D-Wave Systems are designed to solve complex combinatorial optimization problems. It has been shown in literature how to use these QPUs to perform both complex sampling and optimization tasks [37, 40], and how the properties of the quantum bits (qubits) play a role in the computation of solutions. The QPU is designed to solve quadratic unconstrained binary optimization (QUBO) problems, where each qubit represents a variable, and couplers between qubits represent the costs associated with qubit pairs. The QPU is a physical implementation of an undirected graph (G) with qubits as vertices (V) and couplers as edges (E) between them. The functional form of the QUBO that the QPU is designed to minimize is:

$$\text{Obj}(x, Q) = x^T \cdot Q \cdot x, \quad (1)$$

where x is a vector of binary variables of size N , and Q is an $N \times N$ real-valued matrix describing the relationship between the variables. Given the matrix Q , finding binary variable assignments to minimize the objective function in Equation 1 is a known NP-hard problem.

In this paper, we will introduce the traffic flow optimization problem. We start with the T-Drive trajectory dataset¹ of cars’ GPS coordinates, and develop a workflow to mimic a production system that aims to optimize traffic flow in real time. We show how to transform key elements of the problem to QUBO form, for optimization on the D-Wave system (including both the machine and software tools that use it). We treat the D-Wave system as an optimization black box, and show that it is possible to integrate D-Wave QPU calls into a workflow that resembles a real-world application.

2 Formulation of the traffic flow problem

The objective of the traffic flow optimization problem is to minimize the time for a given set of cars to travel between their individual sources and destinations, by minimizing total congestion over all road segments. Congestion on an individual segment is determined by a quadratic function of the number of cars traversing it in a specific time interval. To ensure reproducibility, we used the publicly available T-Drive trajectory dataset containing trajectories of 10,357 taxis recorded over one week. The dataset features 15 million data points, and the total distance of the trajectories makes up about 9 million kilometers [16–18]. To mimic a production system, we required every car to transmit its GPS coordinates in intervals of 1 to 5 seconds. Because not all cars in the dataset provide transmission data at this rate, we enriched the dataset by interpolating between GPS points. We split the problem into a step-by-step workflow, outlined below. “Classical” refers to calculations on classical machines, and “quantum” refers to calculation on the D-Wave system:

¹This open source dataset provided by Microsoft can be found here:
<https://www.microsoft.com/en-us/research/publication/t-drive-trajectory-data-sample/>

1. Classical: Pre-process map and GPS data for use in the online computation.
2. Classical: Predict areas where traffic flow congestion occurs, 15 minutes ahead of time. Areas of congestion are known as hot spots.
3. Classical: Determine spatially and temporally valid alternative routes for each car in the dataset, if possible.
4. Classical: Formulate the minimization problem as a QUBO (to minimize congestion in road segments on overlapping routes).
5. Hybrid Quantum/Classical: Find a solution that minimizes congestion (not necessarily optimally) among route assignments in the whole traffic graph.
6. Classical: Redistribute the cars based on the results.
7. Iterate over steps 2 to 6 until no traffic congestion for the given time window is predicted.

2.1 Classical prediction of hot spots

As part of the pre-processing step in the workflow described in the previous section, we train a classifier (classically) to predict traffic flow hot spots (congestion) throughout the traffic graph. We do this by applying a survival data mining approach:

1. Divide the roads into segments $S = s_1, s_2, \dots, s_n$.
2. Define overlapping time windows $T = \{t_{0\dots m}, t_{n\dots 2m}, t_{2m\dots 3m}, \dots\}$.
3. Train a classifier on the patterns causing hot spots 15 minutes before hot spots occur.

The classifier predicting the hot spots was defined as a convolutional neural network with weight decay regularization, Rectified Linear Units (ReLU) [19], Batch Normalization [20], dropout [21], stochastic gradient descent with Nesterov momentum [22], gradient clipping [23], and learning rate scheduling [24], and softmax [25] activation in the output layer. The output of the network is given by two neurons, the first estimating the probability of a traffic jam occurring, and the second estimating the probability that no traffic jam will occur. A visualization of the input graph is shown in Figure 1. This visualization was generated using the OSMnx API, which is based on OpenStreetMap and allows for retrieving, constructing, analyzing, and visualizing street networks from OpenStreetMap [26].

2.2 Determination of alternate routes

To illustrate how we formulate the problem, we focus on a subset of the T-Drive dataset. Of the 10,357 cars in the dataset, we select 418 of those that are traveling to or from the city center and the Beijing airport. Of course, it is trivial to extend this to all cars, but we use this limited subset to highlight the problem formulation. In this specific scenario, the goal was to redirect a subset of the 418 cars to alternative routes such that the traffic flow on the initial and target routes is maximized (meaning, time from source to target for each car is minimized). For this, optimizing over all cars simultaneously is required, which means that any redistribution of cars that resolves the original hot



Figure 1: OSMnx graph for the downtown-area of Beijing [26]

spot must not cause a traffic jam anywhere else in the map. We used the OSMnx package to split the map of Beijing into segments and nodes, and assign a unique ID to each. Our procedure can be summarized as follows:

1. Extract the road graph from the Beijing city map using OSMnx. This returns lists of segments and nodes with IDs. Nodes represent intersections of segments, and segments are edges connecting the nodes, representing the streets (Figure 1).
2. Map the T-Drive trajectory dataset GPS coordinates for the taxis onto street segments in the graph, to determine the routes taken by the cars.
3. For each car ID and each source and destination node, we extract all simple paths from source to destination, and obtain three candidate alternative routes.

We use these three candidates as proposed alternative routes to redistribute traffic. A full derivation and explanation of these steps is outlined in the appendix (Section A).

2.3 Formulating the traffic flow optimization in QUBO form

The definition of variables for the QUBO (Equation 1) requires some classical pre-processing on the input. Keeping in mind that the traffic flow optimization should mimic a real-life production system, in rare cases it may not be possible to switch a car to different route in the given time window. For example, if there is no intersection or ramp near the car, it will not be considered for rerouting and will remain on its original path. Nevertheless, this car will still affect possible routings of other cars, so it is included in the QUBO. Figure 2 shows an example with road segments assigned to a car ID, as it is used in our workflow. To optimize the traffic flow, we minimize the number of overlapping segments between assigned routes for each car per time slice. Thus, we formulate the optimization problem as follows: “Given three possible routes per car, which assignment of cars to routes minimizes the overall congestion on all road segments?” This is done by requiring that every

```
{10012: [[30888192,146612995,25006941,342687925,190
375162,1903751,175388762,146612956,169587517],
[30888192,169707874,146612995,25006941,169707825,34
2687925,190375162,190375161,175388762,146612956,169
587517],...]}
```

Figure 2: An example of a single car (with ID 10012) and its assigned routes, split into segments.

car be assigned one of the three possible routes, while simultaneously minimizing total congestion over all assigned routes. It is important to emphasize that in this example, as presented at the CeBIT 2017 conference [33], each car was proposed 3 possible alternative routes — not the same set of 3 routes for all cars. This not need be the case in general; cars can have many possible routes. In this example we take (maximum) 3 routes per car for simplicity, because the mathematical description of the problem is identical regardless of the number of routes.

For every possible assignment of car to route, we define a binary variable q_{ij} representing car i taking route j . We define a constraint such that every car is required to take exactly one route; because each car can only occupy one route as a time, exactly one variable per car must be turned on in the minimum of the QUBO. This can be formulated as the following constraint (assuming 3 possible routes):

$$\left(\sum_{j \in \{1,2,3\}} q_{ij} - 1 \right)^2 = -q_{i1} - q_{i2} - q_{i3} + 2q_{i1}q_{i2} + 2q_{i2}q_{i3} + 2q_{i1}q_{i3} + 1, \quad (2)$$

simplified using the binary rule $x^2 = x$. As stated previously, routes are described by lists of street segments (S being the set of all street segments in the graph). Therefore, for all cars i , with proposed routes $j \in \{1, 2, 3\}$, which share the street segment $s \in S$, the cost of the occupancy of the street segment is given by:

$$\text{cost}(s) = \left(\sum_i \sum_j \sum_{s \in j} q_{ij} \right)^2 \quad (3)$$

The global cost function can now be simply described by summing the cost functions for each street segment and the constraint from Equation 2:

$$\text{Obj} = \sum_s^S \text{cost}(s) + \sum_i \lambda_i \left(\sum_j q_{ij} - 1 \right)^2. \quad (4)$$

When summing up components of the global cost function, scaling parameter λ_i is introduced. This ensures that the respective contributions of the components to the cost function do not permit infeasible solutions to the problem in the minimum of the QUBO. To find this scaling factor, we count the number of other constraints in the problem, and use this value as the scale. This makes the cost of violating Equation 2 greater than the cost of violating any other constraint in the QUBO. In this paper, we use the same scaling factor for all λ_i in Equation 4, for simplicity.

Now the cost function can be formulated as a quadratic, upper-triangular matrix, as required for the QUBO problem. We keep a mapping of binary variable q_{ij} to index in the QUBO matrix, given by $I(i, j)$. These indices are the diagonals of the QUBO matrix. The elements of the matrix are the coefficients of the terms in the cost function. To add these elements to the QUBO matrix, whenever two routes j and j' share a street segment s :

1. We add a (+1), linear in the binary variable (at diagonal index $I(i, j)$), for every car i proposed with route j containing segment s .
2. We add a quadratic mixed term (+2), for every pair of cars i_1 and i_2 taking route j containing segment s ($2q_{i_1 j}q_{i_2 j}$ is the off-diagonal element given by indices $I(i_1, j)$ and $I(i_2, j)$).

We then add the constraints to enforce that every car has only one route, as per Equation 2:

1. For every car i with possible route j , we add $(-\lambda_i)$ to the diagonal of the QUBO given by index $I(i, j)$.
2. For every cross-term arising from Equation 2, we add $(2 \cdot \lambda_i)$.

{20050: [541, 542, 543],...}

Figure 3: Car ID 20050 mapped to qubits 541, 542, 543.

Unique car IDs and their mapping $I(i, j)$ to qubits are kept in memory, as shown in Figure 3. A special case occurs if a car is proposed only one route, meaning $q_{ij} = 1$. However, as stated previously, despite car i being assigned to route j , this assignment still affects other cars. This forces the quadratic constraint terms from Equation 3 to be turned into additional linear terms: $2q_{ij}q_{i'j'} \rightarrow 2q_{i'j'}$.

Additionally, by keeping a record of which routes every segment appears in, we can remove the redundant constraints, as some routes may overlap in more than one segment. This results in a QUBO matrix as shown in Figure 4.

[-2918	5864	12	...	0	0	0]
[0	-2908	8	...	0	0	0]
[0	0	-2920	...	0	0	0]
...							
[0	0	0	...	-2925	5854	5854]
[0	0	0	...	0	-2924	5856]
[0	0	0	...	0	0	-2924]

Figure 4: QUBO matrix describing the traffic flow problem (as shown at CeBIT 2017).

In the example presented, we proposed 418 cars with 3 possible routes. Of course, we are not limited to 418 cars in practice, as by iterative execution of the algorithm on newly predicted hot spots, we achieve equilibrium over time. After the redistribution of cars, given the predicted hot spots,

we classically predict hot spots given the new situation and optimize the vehicles in the new target zone.

The 418-car example used 1254 logical variables to represent the problem. A challenge in this scenario is the restricted connectivity between qubits, which limits the ability to directly solve arbitrarily-structured problems. When using the D-Wave QPU directly, an interaction between two problem variables can only occur when there is a physical connection (coupler) between the qubits representing these variables. For most problems, the interactions between variables do not match the QPU connectivity. This limitation can be circumvented using minor-embedding, a technique that maps one graph structure to another. However, this requires finding an embedding that maps to the QPU topology before solving the problem. Finding such an embedding is itself a hard optimization problem [27]. The QPU we used has 1135 functional qubits, thus it was not possible to embed the 418 car example on the QPU at once. Therefore, the problem was solved using the hybrid classical/quantum tool `qbsolv` (described in the next section).

Expressed as pseudo-code, the important high-level steps of the traffic flow optimization algorithm are as follows:

1. Do forever: predict hot spots $H = \{h_1, \dots, h_n\}$ classically 15 minutes before they occur.
2. If $H \neq \{\}$, for each hot spot h :
 - (a) For each car i
 - i. Determine the current route j .
 - (b) For each route j_i
 - i. Map the source j_{i_s} and destination j_{i_d} to their nearest nodes in the road graph.
 - (c) For each j with source and destination $\{j_s, j_d\}$:
 - i. Determine all simple paths from source to destination.
 - ii. Find two alternative paths that are maximally dissimilar to j and to each other.
 - (d) For each car i , define the set of possible routes needed to form the QUBO.
 - (e) Define the QUBO with binary variables q_{ij} by setting the cost per street segment per Equation 3, and applying the constraint in Equation 2.
 - (f) If a car i is given only one route:
 - i. Set $q_{ij} = 1$
 - ii. Turn mixed term into an additional linear term for the other car in the pair taking that route: $2q_{ij}q_{i'j'} \rightarrow 2q_{i'j'}$
 - (g) Solve the QUBO problem using `qbsolv`.
 - (h) Update cars with the selected routes as provided by `qbsolv`.

2.4 Simplified traffic flow

The careful reader will see that we have greatly simplified the concept of real-world traffic flow, by only taking into consideration routes taken by cars. For simplicity, our initial implementation of the traffic

flow optimization problem (to be solved using a QPU) considered only motion data of a subset of agents contributing to traffic, captured by GPS-signals transmitted by cars. Although this distribution of agents (i.e., cars) allows us to understand the traffic situation at a given time, redistribution without considering all agents may not maximally improve the traffic situation, especially for the agents we do not have access to. Other agents contributing to traffic flow could include the following: public transportation, pedestrians, cyclists, and infrastructure. It is important to emphasize that the project highlighted in this paper is an initial attempt at mapping traffic flow optimization to a QUBO formulation, but, as presented, is not the final implementation. We also note that using the experience and knowledge gained throughout this project, we can extend our formulation of the traffic flow optimization as a QUBO problem to also include these additional agents in the future. How to implement this is the subject of current and future research.

3 Review of the D-Wave solvers and architecture

Here, we briefly introduce the solvers and tools provided by D-Wave, to help understand how the problem was solved using the QPU.

3.1 Connectivity and topology

The topology of the D-Wave 2X QPU is based on a C_{12} Chimera graph containing 1152 vertices (qubits) and over 3000 edges (couplers). A Chimera graph of size C_N is an $N \times N$ grid of Chimera cells (also called unit tiles or unit cells), each containing a complete bipartite graph of 8 vertices ($K_{4,4}$). Each vertex is connected to its four neighbors inside the cell as well as two neighbors (north/south or east/west) outside the cell: therefore every vertex has degree 6 excluding boundary vertices [30].

Given the sparse connectivity of current-generation QPUs, in order to solve generic graph structures on the QPU, we must find a graph minor-embedding to fit the topology of the QPU. However, there are multiple issues with solving problems with direct embedding. First, are still limited by the number of qubits on the QPU. Second, embedding is a time-consuming process which requires heuristic approaches in itself, as finding optimal embeddings is NP-hard. Additionally, due to fabrication and calibration issues, some qubits within the QPU may not be operational. This makes it more difficult to embed problems efficiently. To combat the QPU yield issues, D-Wave has recently introduced a “virtual full-yield Chimera” (VFYC) solver, which takes the working QPU and simulates the missing qubits and couplers using classical software. While this method is not equal to having a full-yielded physical QPU, this allows for some programs to be standardized across the different QPUs, and within generations of QPUs. It is then possible to use hybrid classical/quantum approaches (such as the `qbsolv` algorithm, presented next) to solve large, generic problems. This VFYC version of the D-Wave 2X solver was used in our experiments.

3.2 The `qbsolv` algorithm

In January 2017, D-Wave Systems open-sourced the software tool `qbsolv` [38]². The purpose of this algorithm is to provide the ability to solve larger QUBO problems, and with higher connectivity, than is currently possible on the QPU. Given a large QUBO input, `qbsolv` partitions the input into important components and then solves the components independently using queries to the QPU. This process iterates (with different components found by Tabu search) until no improvement in the solution is found. The `qbsolv` algorithm can optimize sub-problems using either a classical Tabu solver or via submission to a D-Wave QPU. In this paper, we run `qbsolv` in the hybrid classical/quantum mode of submitting sub-problems to the D-Wave 2X QPU.

The high-level steps performed by `qbsolv` in hybrid mode are as follows:

1. Find the largest clique³ that can be minor embedded in the QPU topology, or in the full Chimera graph if using the VFYC feature. This one-time operation can be done in advance.
2. Given a QUBO problem, initialize random bit-string representing a solution to the problem.
3. Use a heuristic method to rank nodes according to importance; create a subproblem that fits on the QPU using the importance ranking.
4. Create sub-problem using the importance order.
5. Solve sub-problem by submitting it to the QPU and update variable states in the bit-string.
6. Iterate steps 3 to 5 until no improvement in the objective function is found.

In Section 4 we explain how we executed `qbsolv` on our input problem and interpret the results obtained. A full description of how the `qbsolv` algorithm works is detailed in [39].

3.3 SAPI

The Solver Application Programming Interface (SAPI) is a software library provided by D-Wave Systems that allows communication directly with the QPU and other solvers. Many functions, such as embedding problems and unembedding solutions, are included in the library. Our program used SAPI primarily to create local and remote connections, and to access local and remote solvers. Furthermore, it allows us to examine the solver properties and parameters, and create the correct data structures for the call to the QPU.

4 Results

Our first and foremost goal was to show that we can obtain relevant solutions to a real-world problem using quantum annealing. In this scenario we are not necessarily concerned with finding optimal solutions, which may require unacceptably long run-times; instead we require good quality solutions found within short runtime limits. To evaluate the quality of a solution, we count the number of

²The source code can be found at: github.com/dwavesystems/qbsolv

³A clique is a graph where all nodes are connected to each other.

congested roads after optimization. To do this we simply count the number of segments that intersect (between routes) more than a given number of times, $N_{\text{intersections}}$. For this experiment, we chose $N_{\text{intersections}} = 10$.

To evaluate the QUBO formulation of the traffic flow problem, we designed the following experiment: for the 418 car QUBO problem (as presented in Section 2.3), we solve the problem 50 times using `qbsolv`. We also generate 50 random assignments of cars to routes as reference for the results. In Figure 5 we show the distribution of results (measured as the number of congested segments) after running the experiments using `qbsolv` and random assignments.

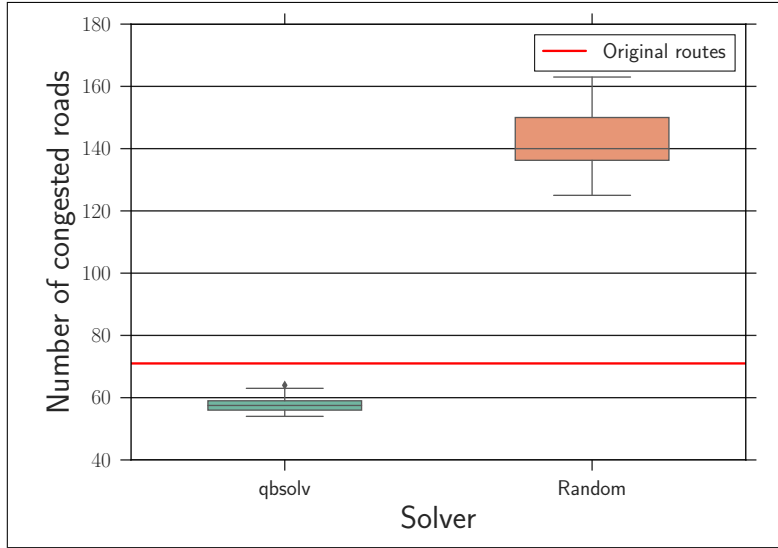


Figure 5: Results comparing random assignment of cars to routes and `qbsolv`. The y-axis shows the distribution of number of congested roads. The red line is the number of congested roads given the original assignments of routes.

From the results in Figure 5, we can see that `qbsolv` redistributes the traffic over possible routes in a way that reduces the overlap between the routes. This is evident both with respect to random assignment of routes, and also shows improvement over the original assignment of routes. It should be noted that in the original assignment, there was a relatively small number of streets that are heavily occupied (meaning above the $N_{\text{intersections}} = 10$ threshold), as all the cars shared the same route, and that the average occupancy was much higher than $N_{\text{intersections}} = 10$. It is also worth noting that all 50 experiments using `qbsolv` resolved the congestion.

One of the main concerns of this paper is demonstrating the ability to perform the traffic optimization in a time-sensitive manner. To show this, we measure the performance of `qbsolv` as a function of the run-time of `qbsolv`. The `qbsolv` source code was compiled and executed on a local D-Wave server in Burnaby, Canada, to minimize the latency between submitting jobs to the QPU and obtaining the results. However, since the QPU used was a shared resource via the cloud, run-time

of `qbsolv` was limited by the job queue for the D-Wave 2X. This caused the observed run-times to range between 22 to 851 seconds. Therefore, we consider the run-time of `qbsolv` to be minimum of the observed run-times, as this represents most faithfully the algorithm, independent of the load on the D-Wave system. This run-time was observed as 22 seconds. There is also no evidence of correlation between the run-time of `qbsolv` and performance (as stated, the long run-times are due to waiting in the job submission queue). In the context of mimicking a production-level application, and given the timing and performance results of `qbsolv`, it is reasonable to assume that a dedicated D-Wave QPU (circumventing the public job submission queue) would be suitable for this kind of application. A visual showing the hot spots of traffic on the Beijing road graph before (original routes) and after optimization (using `qbsolv`) is shown in Figure 6.

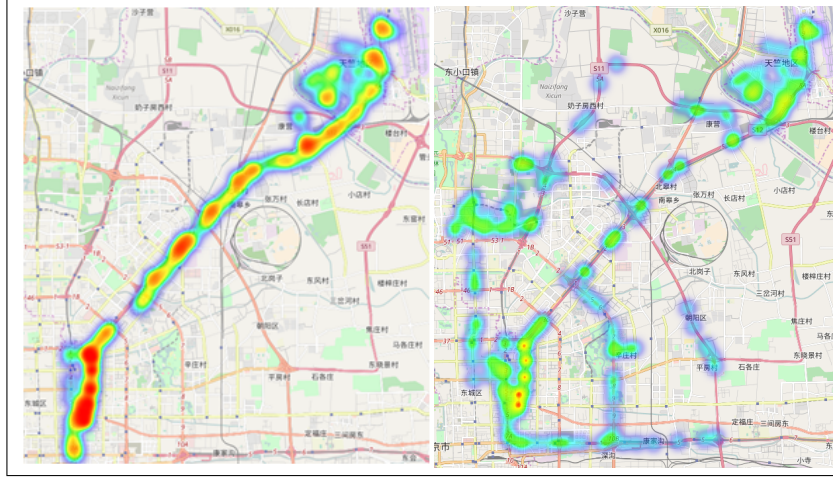


Figure 6: Left: Unoptimized situation under consideration of cars causing traffic jam in the network. Right: Optimized re-distributed cars using `qbsolv`. Note that the areas in red, which indicate congestion, are mostly absent from the right picture.

5 Conclusions and future work

The currently presented problem is a simplified version of traffic flow, as it incorporates only a limited set of cars, no communication to infrastructure, no other traffic participants, and no other optimization targets except minimization of time from source to destination. In our future work, we intend to consider all of these parameters, and will also need to consider creative ways of formulating these parameters as part of the QUBO problem. We will continue to focus on solving real-world problems by means of quantum machine learning [34–36], quantum simulation, and quantum optimization. Furthermore, we find that these types of real-time optimization problems are well-suited for the D-Wave systems, and the hybrid tools that use them. The more combinatorially complex the problem becomes, in future developments, the more time is needed for classical algorithms to consider additional parameters. However, D-Wave QPUs have historically grown in number of qubits from one generation to the next, and given that this trend is likely to continue, it is reasonable to assume that obtaining high-quality solutions quickly using the QPU will be sustainable moving forward.

Acknowledgments

Thanks go to VW Group CIO Martin Hofmann and VW Group Region Americas CIO Abdallah Shanti, who are always open to new technologies, and who enabled this project. Further thanks go to the team at D-Wave, who were particularly supportive and helped us understand how to leverage the full capacity of their systems, especially to Murray Thom, Adam Douglass, and Andy Mason.

References

- [1] D-Wave (2017): Quantum Computing, How D-Wave Systems Work [04-24-2017]; URL: <https://www.dwavesys.com/quantum-computing>
- [2] M. Benedetti, J.R.-Gómez, R. Biswas, A. Perdomo-Ortiz (2015): Estimation of effective temperatures in a quantum annealer and its impact in sampling applications: A case study towards deep learning applications; URL: <https://arxiv.org/abs/1511.02581>
- [3] V. N. Smelyanskiy, D. Venturelli, A. Perdomo-Ortiz, S. Knysh, M. I. Dykman (2015): Quantum annealing via environment-mediated quantum diffusion; URL: <https://arxiv.org/abs/1511.02581>
- [4] D. Venturelli, D. J.J. Marchand, G. Rojo (2015): Quantum Annealing Implementation of Job-Shop Scheduling; URL: <https://arxiv.org/abs/1506.08479>
- [5] Z. Jiang, E. G. Rieffel (2015): Non-commuting two-local Hamiltonians for quantum error suppression; URL: <https://arxiv.org/abs/1511.01997>
- [6] S. V. Isakov, G. Mazzola, V. N. Smelyanskiy, Z. Jiang, S. Boixo, H. Neven, M. Troyer (2015): Understanding Quantum Tunneling through Quantum Monte Carlo Simulations(2015); URL: <https://arxiv.org/abs/1510.08057>
- [7] B. O’Gorman, A. Perdomo-Ortiz, R. Babbush, A. Aspuru-Guzik, V. Smelyanskiy (2014): Bayesian Network Structure Learning Using Quantum Annealing; URL: <https://arxiv.org/abs/1407.3897>
- [8] E. G. Rieffel, D. Venturelli, B. O’Gorman, M. B. Do, E. Prystay, V. N. Smelyanskiy (2014): A case study in programming a quantum annealer for hard operational planning problems; <https://arxiv.org/abs/1407.2887>
- [9] D. Venturelli, S. Mandr, S. Knysh, B. O’Gorman, R. Biswas, V. Smelyanskiy (2014): Quantum Optimization of Fully-Connected Spin Glasses; URL: <https://arxiv.org/abs/1406.7553>
- [10] A. Perdomo-Ortiz, J. Fluegemann, S. Narasimhan, R. Biswas, V. N. Smelyanskiy (2014): A Quantum Annealing Approach for Fault Detection and Diagnosis of Graph-Based Systems; URL: <https://arxiv.org/abs/1406.7601>
- [11] S. Boixo, T. F. Ronnow, S. V. Isakov, Z. Wang, D. Wecker, D. A. Lidar, J. M. Martinis, M. Troyer (2014): Quantum annealing with more than one hundred qubits; URL: <https://arxiv.org/abs/1304.4595>
- [12] R. Babbush, A. Perdomo-Ortiz, B. O’Gorman, W. Macready, A. Aspuru-Guzik (2012): Construction of Energy Functions for Lattice Heteropolymer Models: Efficient Encodings for Constraint Satisfaction Programming and Quantum Annealing Advances in Chemical Physics, in press; URL: <https://arxiv.org/abs/1211.3422>
- [13] L. Wang, T. F. Ronnow, S. Boixo, S. V. Isakov, Z. Wang, D. Wecker, D. A. Lidar, J. M. Martinis, M. Troyer (2013): Classical signature of quantum annealing; URL: <https://arxiv.org/abs/1305.5837>

- [14] A. Perdomo-Ortiz, N. Dickson, M. Drew-Brook, G. Rose, A. Aspuru-Guzik (2012): Finding low-energy conformations of lattice protein models by quantum annealing; URL: <https://arxiv.org/abs/1204.5485>
- [15] Los Alamos National Laboratory (2016): D-Wave 2X Quantum Computer; URL: <http://www.lanl.gov/projects/national-security-education-center/information-science-technology/dwave/>
- [16] J. Yuan, Y. Zheng, X. Xie, and G. Sun (2011): Driving with knowledge from the physical world. In The 17th ACM SIGKDD international conference on Knowledge Discovery and Data mining, KDD11, New York, NY, USA. ACM.
- [17] J. Yuan, Y. Zheng, C. Zhang, W. Xie, X. Xie, G. Sun, Y. Huang (2010): T-drive: driving directions based on taxi trajectories. In Proceedings of the 18th SIGSPATIAL International Conference on Advances in Geographic Information Systems, GIS 10, pages 99-108, New York, NY, USA. ACM.
- [18] Microsoft (2011): T-Drive trajectory data sample [4-24-2017]; URL: <https://www.microsoft.com/en-us/research/publication/t-drive-trajectory-data-sample/>
- [19] V. Nair, G. E. Hinton (2010): Rectified linear units improve restricted Boltzmann machines. In Proceedings of the 27th International Conference on Machine Learning (ICML-10), pages 807-814, 2010.
- [20] S. Ioffe, C. Szegedy (2015): Batch normalization: Accelerating deep network training by reducing internal covariate shift. arXiv preprint arXiv:1502.03167.
- [21] N. Srivastava, G. Hinton, A. Krizhevsky, I. Sutskever, R. Salakhutdinov (2014): Dropout: A simple way to prevent neural networks from overfitting. The Journal of Machine Learning Research, 15(1):1929-1958.
- [22] Y. Nesterov et al. (2007): Gradient methods for minimizing composite objective function. Technical report, UCL.
- [23] R. Pascanu, T. Mikolov, Y. Bengio (2012): Understanding the exploding gradient problem. Computing Research Repository (CoRR) abs/1211.5063.
- [24] A. Senior, G. Heigold, M. A. Ranzato, K. Yang (2013): An empirical study of learning rates in deep neural networks for speech recognition. In Acoustics, Speech and Signal Processing (ICASSP), 2013 IEEE International Conference on, pages 6724-6728. IEEE.
- [25] C. M. Bishop (2006): Pattern Recognition and Machine Learning. Springer.
- [26] G. Boeing (2017): OSMnx: New Methods for Acquiring, Constructing, Analyzing, and Visualizing Complex Street Networks. doi:10.2139/ssrn.2865501.
- [27] D-Wave (2016): Developer Guide for Python; D-Wave

- [28] F. Neukart, S.-A. Moraru, C.-M. Grigorescu, P. Szakacs-Simon (2012): Transgenetic NeuroEvolution. Proceedings of OPTIM 2012
- [29] D-Wave (2016): Partitioning Optimization Problems for Hybrid Classical/Quantum Execution [4-28-2017]; URL: https://github.com/dwavesystems/mathttqbsolv/blob/master/mathttqbsolv_techReport.pdf
- [30] J. King et al. (2017): Quantum Annealing amid Local Ruggedness and Global Frustration; arXiv:1701.04579 [quant-ph]
- [31] D. Korenkevych et al. (2016): Benchmarking Quantum Hardware for Training of Fully Visible Boltzmann Machines; arXiv:1611.04528 [quant-ph]
- [32] Lanting, T. et al. (2013): Entanglement in a Quantum Annealing Processor; Phys. Rev. X 4, 021041
- [33] Springer Professional: Volkswagen Trials Quantum Computers; URL: https://www.springerprofessional.de/en/automotive-electronics—software/companies—institutions/volkswagen-trials-quantum-computers/12170146?wt_mc=offsi.emag.mtz-worldwide.rssnews.-.x
- [34] F. Neukart, S. M. Moraru (2013): On Quantum Computers and Artificial Neural Networks; Signal Processing Research 2 (1), 1-11
- [35] F. Neukart, S. M. Moraru (2014): Operations on Quantum Physical Artificial Neural Structures; Procedia Engineering 69, 1509-1517
- [36] J. Biamonte et al. (2016): Quantum Machine Learning; arXiv:1611.09347 [quant-ph]
- [37] J. Raymond, S. Yarkoni, E. Andriyash, “Global Warming: Temperature Estimation in Annealers”, Front. ICT, 07 November 2016
<https://doi.org/10.3389/fict.2016.00023>
- [38] “D-Wave Initiates Open Quantum Software Environment”, press release, D-Wave website.
<https://www.dwavesys.com/press-releases/d-wave-initiates-open-quantum-software-environment>
- [39] M. Booth, S. P. Reinhardt, A. Roy, “Partitioning Optimization Problems for Hybrid Classical/Quantum Execution”, retrieved Jul 19, 2017.
<https://www.dwavesys.com/resources/publications>
- [40] V. S. Denchev, S. Boixo, S. V. Isakov, N. Ding, R. Babbush, V. Smelyanskiy, J. Martinis, H. Neven, “What is the Computational Value of Finite Range Tunneling?”, Phys. Rev. X 6, 031015 (2016).

A Derivation of alternative routes calculation

In this section we detail the mathematics behind the steps in Section 2.2.

A.1 Mapping GPS coordinates to segments

We chose the Haversine-distance (Equations 5-7) for determining the closest nodes to each start and end-coordinate on the graph.

$$a = \sin^2\left(\Delta \frac{lat}{2}\right) + \cos(lat_1) \cos(lat_2) \sin^2\left(\Delta \frac{lon}{2}\right), \quad (5)$$

$$c = 2 \operatorname{atan2}\left(\sqrt{a}, \sqrt{1-a}\right), \quad (6)$$

$$d = Rc, \quad (7)$$

where lat is the latitude, lon the longitude, R the radius of the earth (6,371 km), and d the distance between two points. The function $\operatorname{atan2}$ is the arctangent function taking two arguments, and for the arguments x and y , which are, of course, not both equal to zero, $\operatorname{atan2}(y, x)$ is the angle in radians between the positive x-axis of a plane and the point given by the coordinates (x, y) on it. The angle is positive for counter-clockwise angles, and negative for clockwise angles. The purpose of using two arguments instead of one, i.e. computing a $\operatorname{atan}(\frac{y}{x})$, is to gather information on the signs of the inputs in order to return the appropriate quadrant of the computed angle, which is not possible for the single-argument arctangent function. It also avoids the problem of division by zero, as $\operatorname{atan2}(y, 0)$ will return a valid answer as long as y is non-zero. For any given source and destination coordinate we define a space-window of 1 km around it (source and destination being the center), and calculate the closest node in that space window. For this, a translation of φ and λ into x and y coordinates was required:

$$x = R \cos(\varphi) R \cos(\lambda), \quad (8)$$

$$y = R \cos(\varphi) R \sin(\lambda). \quad (9)$$

For determining the window coordinates, we calculated a square around $P_s = (x, y)$; $S \in \{source, destination\}$. In the example below, the north-eastern corner of the rectangle is calculated by adding northern and eastern distance to P_s :

$$d_\varphi = \frac{d_{north}}{R}, \quad (10)$$

$$d_\lambda = \frac{d_{east}}{R \cos\left(\frac{\pi}{180}\right)}, \quad (11)$$

where d_φ represents the distance in latitude, and d_λ the distance in longitude. d_{north} and d_{east} give the distance to the north and distance to the east in meters. The new longitude and latitude, which in the described case is the north-eastern corner of the space window centered around the source or destination coordinate of a route, we add the distance and convert back to coordinates (Equations 12 and 13).

$$\varphi_{new} = \varphi + d(\varphi) \frac{180}{\pi} \quad (12)$$

$$\lambda_{new} = \lambda + d(\lambda) \frac{180}{\pi} \quad (13)$$

Equations 12 and 13 do, of course, require sign changes when the other three window corners are calculated.

A.2 Calculating possible routes

A simple path can traverse several nodes from source to destination, but without returning to nodes which were already visited (no cycles). Several thousands of simple paths from source to destination (per car) may exist. In our study we selected the two simple paths that are most dissimilar to the original route, and proposed these as alternates, along with the original route. To find the dissimilar routes, we selected routes that share the smallest number of overlapping segments with the original. Our calculation is based on the Jaccard similarity coefficient:

$$J(R, R') = \frac{R \cap R'}{R \cup R'}, \quad (14)$$

where R, R' represent two routes, each considered as a set of segments. The Jaccard distance then tells us which routes are maximally dissimilar to each other:

$$d_J(R, R') = 1 - J(R, R'). \quad (15)$$

Using this, we select two candidates that are the most dissimilar to the original route, and propose these two (plus the original route) as possible redistribution routes.